

# Multi-strategy vertical parking path planning considering the influence of obstacles

Tongqing Zhang\*, Shuai Zhang, Pengcheng Ma, Ruiyuan Liu, Jiaojiao Li

School of Transportation and vehicle engineering, Shandong University of Technology, Zibo 255000, Shandong, China.

\* Corresponding author: Tongqing Zhang.

**Abstract:** For the vertical parking scene with narrow parking spaces, this paper proposes three kinds of path planning strategies to guide the vehicle to park safely and successfully in the parking spaces by using the path planning method of arc-line-mitigation curve and considering the initial posture and position relationship of different vehicles. Then, considering the complexity of the actual parking environment, obstacle analysis and future trajectory prediction of dynamic obstacles are added, and the impact of different obstacles on the parking path is analyzed. Three obstacle avoidance methods are proposed, and three planning strategies are combined to achieve safe and efficient vertical parking. Finally, the path planning method is simulated and verified in QT environment. The results show that the vertical parking path planning method proposed in this paper meets the parking needs of narrow vertical parking spaces and achieves safe and efficient parking with predictability.

**Keywords:** Automatic parking; Path planning; Arc-line-détente curve; Obstacle prediction; Optimal path.

## 1. Introduction

With the rapid growth of motor vehicle ownership, the shortage of traffic resources is becoming more and more serious, and the problems of urban congestion, insufficient parking space and narrow parking space are becoming more and more prominent, resulting in frequent parking safety accidents. Relevant data show that in all kinds of traffic accidents, accidents in parking scenarios account for 44 % of the total [1]. With the increasingly narrow parking space, the requirements for the driver's parking technology are also increasing, and the driver's driving experience is poor. In addition, the number of adjustments and parking time of the driver during the parking process also increases. More than 30 % of the vehicles on the road are in patrol or parking, and the average time spent on parking is more than eight minutes. [2]. Therefore, with the advancement of automobile intelligence, automatic parking technology has developed rapidly. The automatic parking system has greatly improved the safety and efficiency of the parking process, improved the driving experience, and realized safe, efficient and convenient parking.

At present, the research on the path planning part of the automatic parking system is mainly divided into four kinds: one is the geometric method, which has the advantages of smooth path, low model calculation and strong applicability, but the applicability is not strong; the second is the numerical optimization method, which finds the optimal path by considering the constraint optimization problem. This method has strong solving ability, but has problems such as large amount of calculation and poor real-time performance. Third, based on sampling method, this kind of algorithm has strong adaptability, but the curvature is not continuous; the fourth is based on the reinforcement learning method, that is, using the reinforcement learning network to train and plan the parking path. This method has strong applicability and strong solving ability, but the algorithm training is usually difficult to converge, and the actual environment application gap is large.

In addition, in the automatic parking path planning, the influence of obstacles should be considered, that is, the

influence of the position, trajectory and predicted trajectory of obstacles on the parking path. The information of obstacle position and historical trajectory can be obtained directly through perception, but the analysis and prediction of obstacles need further research. At present, the main methods are: model-based prediction, including Markov model, Kalman filter, Gaussian distribution, etc., which has the advantages of simple and intuitive, low complexity, but it is more dependent on model parameters and cannot deal with the prediction of complex scenes. The other is based on data-driven deep learning, including DNN, RNN, LSTM and other methods, with high accuracy and high efficiency.

In this paper, the path planning method of arc-line-gentle curve is used to analyze the path planning problem in vertical parking in detail. Combined with the advantages of geometric model and curvature continuity, three path planning strategy models are established to improve the applicability and planning success rate. Then the prediction of obstacles is added, three obstacle avoidance methods are proposed, and the optimal path is selected to ensure the safe and efficient parking of the vehicle.

## 2. Vertical parking path planning strategy

According to different parking environments and constraints, this paper uses different path planning strategies to plan the parking path.

### 2.1. Establishment of vehicle kinematics model

Vehicles in the parking process, the driving speed is low, so the wheel skid can be ignored. Due to the complex shape of the car body, it is necessary to simplify the shape of the car body into a rectangle, and expand the length and width of the rectangle outwards to facilitate the establishment of the vehicle model and further ensure parking safety. The vehicle kinematics is studied according to Ackerman steering principle, and the schematic diagram is shown in Fig. 1.

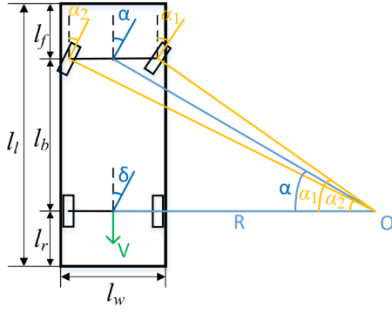


Fig.1 Ackerman turn schematic

The kinematics equation of the vehicle at low speed is:

$$\tan \alpha = \frac{l_b}{R}$$

$$\begin{cases} x_r' = v_r \cdot \cos(\theta) \\ y_r' = v_r \cdot \sin(\theta) \\ \theta' = \frac{v_r}{l_b} \cdot \tan(\alpha) \end{cases}$$

Where,  $\alpha$  is the equivalent front wheel angle;  $l_b$  is the wheelbase of the vehicle;  $r$  is the turning radius of the center point of the vehicle rear axle;  $x_r$  and  $y_r$  are the X and Y axis coordinate values of the center point of the rear axle of the vehicle;  $v_r$  is the speed of the center point of the vehicle rear axle;  $\theta$  is the body posture angle, the angle between the body and the X axis.

## 2.2. Constraint condition analysis

The constraints in the parking process mainly include vehicle kinematics constraints, parking space size constraints, space constraints and obstacle constraints. Obstacle constraints will be analyzed in detail later due to the uncertainty.

### 2.2.1. Vehicle kinematics constraints

In the process of vehicle parking, kinematic constraints mainly consider the maximum angle constraint of vehicle equivalent front wheel and the maximum angle rate constraint of vehicle equivalent front wheel:

$$\begin{cases} \alpha \leq \alpha_{\max} \\ \omega \leq \omega_{\max} \\ R \geq R_{\min} \end{cases}$$

Where,  $\alpha$  represents the equivalent front wheel angle;  $\omega$  represents the equivalent front wheel angle rate;  $r$  denotes the turning radius of the vehicle.

### 2.2.2. Parking space size constraints

The parking space size needs to be larger than the vehicle size to meet the successful parking of the vehicle.

$$\begin{cases} l_l \leq \max\{l_{EG}, l_{EF}\} \\ l_w \leq \min\{l_{EG}, l_{EF}\} \end{cases}$$

In the formula,  $l_l$  is the length of the car,  $l_w$  is the width of the car,  $l_{EG}$  and  $l_{EF}$  are the two sides of the parking space.

### 2.2.3. Spatial constraints

Spatial constraints mainly consider whether the vehicle collides with the spatial boundary, that is, the critical spatial

constraint. Different parking space types have different spatial constraints:

When the vehicle is parked vertically, the left front angle A, right front angle B, left rear angle C, right rear angle D, left and right side I and J of the rear axle are the main collision points. When the key collision points of the above vehicle do not collide with space, the whole vehicle does not collide, which conforms to the space constraint.

$$\begin{cases} y_{A\max} < l_G \cdot y_{B\max} < l_G & (1) \\ y_{C\max} < l_G \cdot y_{D\max} < l_G & (2) \\ -\frac{l_{EF}}{2} < x_{CD} = \frac{y_C \cdot x_D - x_C \cdot y_D}{y_C - y_D} > \frac{l_{EF}}{2} & (3) \\ \text{when: } y_I = 0, x_I \geq -\frac{l_{EF}}{2}; \text{ when: } y_J = 0, x_J \leq \frac{l_{EF}}{2} & (4) \end{cases}$$

Where Formula (1) indicates that the left front corner A and the right front corner C of the vehicle have no collision with the other side of the road; formula (2) indicates that the left rear corner B and the right rear corner D of the vehicle have no collision with the other side of the road; formula (3) indicates that there is no collision between BD behind the vehicle and parking angle E, F. When  $\min(y_B, y_D) \leq 0 \leq \max(y_B, y_D)$ , let  $y = 0$ , the solved  $x$  needs to satisfy formula (4); formula (5) indicates that there is no collision between the left and right sides of the rear axle I, J and the parking angle E, F.

Where, SG represents the width of the road, that is, the longitudinal coordinate value on the other side of the road;  $x_{BD}$  represents the vehicle rear BD; SEF represents the length of the parking space EF.

## 2.3. Parking strategy analysis

Because the environment is changeable when the vehicle is parking vertically, the size of the vehicle and the parking space, the relative position of the vehicle and the parking space, the attitude angle of the vehicle and other parameters are random, so when the vehicle is parking vertically, different parking path planning strategies are needed to realize the successful planning of the safe path and the selection of the efficient path. The parking path planning strategy mainly includes the one-time parking strategy, the reverse parking strategy after the vehicle's forward adjustment and the multiple adjustment parking strategy. The schematic diagrams are shown in Figure 2,3,4, respectively, and are represented by typical scenarios of each parking strategy.

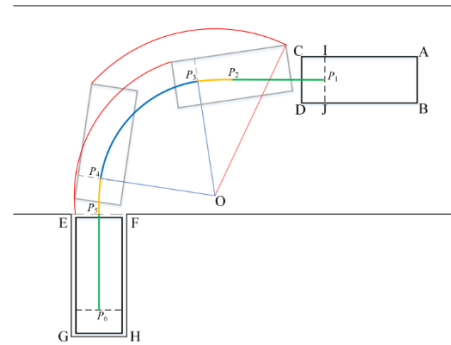
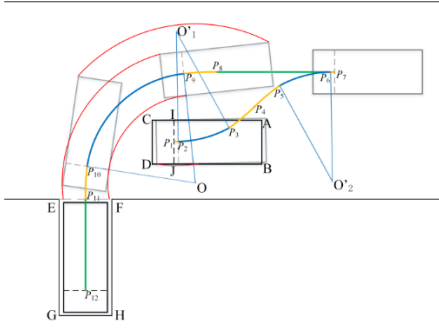
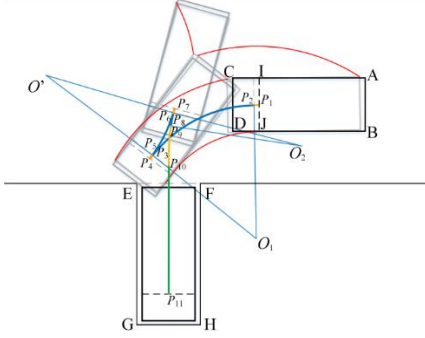


Fig. 2 Trajectory planning of vehicle parking strategy



**Fig. 3** Parking trajectory planning of reverse parking strategy after vehicle forward adjustment



**Fig. 4** Parking Trajectory Planning of Multiple Adjusted Parking Strategy

In the vertical parking path, it mainly includes three-line segments: straight line, arc and transition curve. The formula expression is similar. Therefore, this paper takes the one-time reverse parking strategy as an example to derive and analyze the formula, that is, the following analysis and calculation are carried out for Figure 2.2.

The vehicle parking path consists of straight line P1P2, transition curve P2P3, arc P3P4, transition curve P4P5 and straight line P5P6. wherein, the green line segment represents the straight reversing path of the rear axle center of the vehicle; yellow curve represents the center of the vehicle rear axle ease curve path; the blue curve represents the arc path of the vehicle rear axle center; the red arc represents the vehicle space constraint critical.

(1) Derivation of straight line P1P2:

Let the time-consuming phase of the straight line P1P2 be tP1-tP2 and the distance be lP1P2. When tP1 = 0 ≤ t ≤ tP2, P is a point on the straight line at time t, then the linear equation is:

$$\begin{cases} x_p = x_{p_1} - l_{p_1p} \cdot \cos \theta_{p_1} \\ y_p = y_{p_1} - l_{p_1p} \cdot \sin \theta_{p_1} \\ \theta_p = \theta_{p_1} \end{cases}$$

Where, lP1P denotes the distance from P1 to P,

The intersection point P2 coordinates of the straight line and the transition curve and the body attitude angle are:

$$\begin{cases} x_{p_2} = x_{p_1} - l_{p_1p_2} \cdot \cos \theta_{p_1} \\ y_{p_2} = y_{p_1} - l_{p_1p_2} \cdot \sin \theta_{p_1} \\ \theta_{p_2} = \theta_{p_1} \end{cases}$$

(2) Transition curve P2P3 derivation

The time-consuming stage of the transition curve P2P3 is tP2-tP3. When tP2 < t ≤ tP3, P is a point on the transition curve at time t.

Firstly, according to the theoretical equation of the

transition curve, it can be obtained that:

$$\begin{cases} dx_{p_2p} = l_{p_2p} \left( 1 - \frac{l_{p_2p}^4}{40R_{p_3}^2 l_{p_3}^2} + \frac{l_{p_2p}^8}{3456R_{p_3}^4 l_{p_3}^4} - \frac{l_{p_2p}^{12}}{599040R_{p_3}^6 l_{p_3}^6} + \dots \right) \\ dy_{p_2p} = \frac{l_{p_2p}^3}{6R_{p_3} l_{p_3}} \left( 1 - \frac{l_{p_2p}^4}{56R_{p_3}^2 l_{p_3}^2} + \frac{l_{p_2p}^8}{7040R_{p_3}^4 l_{p_3}^4} - \frac{l_{p_2p}^{12}}{1612800R_{p_3}^6 l_{p_3}^6} + \dots \right) \\ \tau_{p_2p} = \frac{l_{p_2p}^2}{2R_{p_3} l_{p_3}} \end{cases}$$

Where, dxP2P is the longitudinal variation from point P2 to point P, dyP2P is the transverse variation from point P2 to point P, τP2P is the tangential angle variation from point P2 to point P, lP2P is the curve length from point P2 to point P, Rp3 and lp3 are the curvature radius of point P3 and the curve length of P2P3 respectively.

The specific equation of the mitigation curve P2P3 is :

$$\begin{cases} x_p = x_{p_2} - (dx_{p_2p} \cdot \cos \theta_{p_2} - dy_{p_2p} \cdot \sin \theta_{p_2}) \\ y_p = y_{p_2} - (dx_{p_2p} \cdot \sin \theta_{p_2} + dy_{p_2p} \cdot \cos \theta_{p_2}) \\ \theta_p = \theta_{p_2} + \tau_{p_2p} \end{cases}$$

The P3 coordinates of the intersection of the transition curve and the arc and the body attitude angle are :

$$\begin{cases} x_{p_3} = x_{p_2} - (dx_{p_2p_3} \cdot \cos \theta_{p_2} - dy_{p_2p_3} \cdot \sin \theta_{p_2}) \\ y_{p_3} = y_{p_2} - (dx_{p_2p_3} \cdot \sin \theta_{p_2} + dy_{p_2p_3} \cdot \cos \theta_{p_2}) \\ \theta_{p_3} = \theta_{p_2} + \tau_{p_2p_3} \end{cases}$$

(3) Derivation of arc P3P4

Let the radius of P3P4 be R and the time-consuming stage be tP3-tP4. When tP3 < t ≤ tP4, and P is a point on the arc curve at time t.

Firstly, according to the arc theory, we can get:

$$\begin{cases} dox_{p_3p} = R \cdot \sin \beta_p \\ doy_{p_3p} = R \cdot (1 - \cos \beta_p) \\ \beta_{p_3p} = \frac{l_{p_3p}}{R} = \frac{\int_{t_{p_3}}^t v dt}{R} \end{cases}$$

Where, dxP3P is the longitudinal variation from P3 point to P point, dyP3P is the transverse variation from P3 point to P point, βP3P is the central angle variation from P3 point to P point, lP3P is the arc length from P3 point to P point.

The specific equation of the arc curve P3P4 is:

$$\begin{cases} x_p = x_{p_3} - (dox_{p_3p} \cdot \cos \theta_{p_3} - doy_{p_3p} \cdot \sin \theta_{p_3}) \\ y_p = y_{p_3} - (dox_{p_3p} \cdot \sin \theta_{p_3} + doy_{p_3p} \cdot \cos \theta_{p_3}) \\ \theta_p = \theta_{p_3} + \beta_{p_3p} \end{cases}$$

The intersection point P4 coordinates of the arc and the transition curve and the body attitude angle are:

$$\begin{cases} x_{p_4} = x_{p_3} - (dox_{p_3p_4} \cdot \cos \theta_{p_3} - doy_{p_3p_4} \cdot \sin \theta_{p_3}) \\ y_{p_4} = y_{p_3} - (dox_{p_3p_4} \cdot \sin \theta_{p_3} + doy_{p_3p_4} \cdot \cos \theta_{p_3}) \\ \theta_{p_4} = \theta_{p_3} + \beta_{p_3p_4} \end{cases}$$

(4) Transition curve P4P5 derivation

The time-consuming stage of the transition curve P4P5 is tP4-tP5. When tP4 < t ≤ tP5, P is a point on the transition curve at time t.

Since the starting point of the transition curve P4P5 is P4,

the coordinates of the end point P5 of the transition curve can be calculated, and the transition curve equation can be derived and calculated by P5 point. Since the length of the transition curve P4P5 is determined,  $IP4P5 = IP5P4$ , according to the theoretical equation of the transition curve, we can get:

$$\begin{cases} dx_{p_4p_5} = l_{p_4p_5} \left( 1 - \frac{l_{p_4p_5}^2}{40R_{p_4}^2} + \frac{l_{p_4p_5}^4}{3456R_{p_4}^4} - \frac{l_{p_4p_5}^6}{599040R_{p_4}^6} + \dots \right) \\ dy_{p_4p_5} = \frac{l_{p_4p_5}^2}{6R_{p_4}} \left( 1 - \frac{l_{p_4p_5}^2}{56R_{p_4}^2} + \frac{l_{p_4p_5}^4}{7040R_{p_4}^4} - \frac{l_{p_4p_5}^6}{1612800R_{p_4}^6} + \dots \right) \\ \tau_{p_4p_5} = \frac{l_{p_4p_5}}{2R_{p_4}} = \frac{\int_{t_{p_4}}^{t_{p_5}} v dt}{2R_{p_4}} \end{cases}$$

Where,  $dxp5$  is the longitudinal variation from P4 to P5,  $dyp5$  is the transverse variation from P4 to P5,  $\tau p5$  is the tangential angle variation from P4 to P5,  $lp5$  is the curve length from P4 to P5,  $RP4$  is the radius of curvature of P4.

Considering the body attitude angle, the position coordinates of the P5 point of the transition curve are:

$$\begin{cases} x_{p_5} = x_{p_4} - (dx_{p_4p_5} \cdot \cos \theta_{p_4} - dy_{p_4p_5} \cdot \sin \theta_{p_4}) \\ y_{p_5} = y_{p_4} - (dx_{p_4p_5} \cdot \sin \theta_{p_4} + dy_{p_4p_5} \cdot \cos \theta_{p_4}) \\ \theta_{p_5} = \theta_{p_4} + \tau_{p_4p_5} \end{cases}$$

The specific equation of the mitigation curve P4P5 is:

$$\begin{cases} x_p = x_{p_5} + (dx_{p_5p} \cdot \cos \theta_{p_5} - dy_{p_5p} \cdot \sin \theta_{p_5}) \\ y_p = y_{p_5} + (dx_{p_5p} \cdot \sin \theta_{p_5} + dy_{p_5p} \cdot \cos \theta_{p_5}) \\ \theta_p = \theta_{p_5} - \tau_p \end{cases}$$

(5) Straight line P5P6 derivation

The time-consuming stage of the straight line P5P6 is  $tP5-tP6$ , and the distance is  $IP5P6$ . When  $tP5 < t \leq tP6$ , P is a point on the straight line at time t, then the linear equation is:

$$\begin{cases} x_p = x_{p_5} - l_{p_5p} \cdot \cos \theta_{p_5} \\ y_p = y_{p_5} - l_{p_5p} \cdot \sin \theta_{p_5} \\ \theta_p = \theta_{p_5} \end{cases}$$

Where  $IP5P$  denotes the length of a line from P5 to P.

The straight end point P6 coordinates and body attitude angle are:

$$\begin{cases} x_{p_6} = x_{p_5} - l_{p_5p_6} \cdot \cos \theta_{p_5} \\ y_{p_6} = y_{p_5} - l_{p_5p_6} \cdot \sin \theta_{p_5} \\ \theta_{p_6} = \theta_{p_5} \end{cases}$$

In order to ensure the parking quality, the vehicle stops at the center of the parking space after parking, that is, when the parking stops, the coordinates of the P6 position of the vehicle rear axle end point are  $(0, -(\text{SEG} + e) / 2)$ , and the body attitude angle  $\theta p6 = \pi / 2$ .

In addition, the abscissa value of the center O is:

$$x_{p_o} = x_{p_5} + dx_{p_4p_5} + R \cdot \cos \tau_{p_4p_5}$$

$$x_{p_1} - x_{p_o} = l_{p_1p_2} \cdot \cos \theta_{p_1} + (dx_{p_2p_3} \cdot \cos \theta_{p_2} - dy_{p_2p_3} \cdot \sin \theta_{p_2}) - R \cdot \sin(\theta_{p_2} + \tau_{p_2p_3})$$

Therefore, line  $IP1P2$ , line  $IP5P6$  satisfy the following relationship:

$$l_{p_1p_2} = \frac{[x_{p_1} - dx_{p_4p_5} - R \cdot \cos \tau_{p_4p_5} - (dx_{p_2p_3} \cdot \cos \theta_{p_2} - dy_{p_2p_3} \cdot \sin \theta_{p_2}) + R \cdot \sin(\theta_{p_2} + \tau_{p_2p_3})] / \cos \theta_{p_1}}{1}$$

$$l_{p_5p_6} = y_{p_1} - l_{p_1p_2} \cdot \sin \theta_{p_1} - (dx_{p_2p_3} \cdot \sin \theta_{p_2} + dy_{p_2p_3} \cdot \cos \theta_{p_2}) - (dx_{p_3p_4} \cdot \sin \theta_{p_3} + dy_{p_3p_4} \cdot \cos \theta_{p_3}) - (dx_{p_4p_5} \cdot \sin \theta_{p_4} + dy_{p_4p_5} \cdot \cos \theta_{p_4}) + \frac{S_{EG} + e}{2}$$

### 3. Optimal vertical parking path planning considering the influence of obstacles

In the process of vertical parking, it is also necessary to consider the collision constraints of obstacles to ensure that vehicles can park safely. In addition, when the vehicle plans a path that can be safely parked, it is necessary to consider the parking efficiency, that is, the time-consuming of the entire parking process, to achieve the optimal vertical parking path planning.

#### 3.1. Obstacle and collision analysis

##### 3.1.1. Obstacle analysis

Obstacles mainly include static obstacles and dynamic obstacles. Static obstacles mainly consider their position, shape and size. Dynamic obstacles not only consider the above parameters, but also consider their trajectory and predicted trajectory.

(1) The location and size of the obstacle

The shape of the obstacle is simplified to convex polygon or circle, and the side length of the convex polygon or the diameter of the circle is expanded outward  $le$  to realize the model establishment of the irregular shape obstacle and the further guarantee of the parking safety.

Therefore, the convex polygon obstacle can be expressed as:

$$Q_i = \{Q_{i1}Q_{i2}Q_{i3} \dots Q_{i(j-1)}Q_{ij}\} = \{\overline{Q_{i1}Q_{i2}}, \overline{Q_{i2}Q_{i3}}, \dots, \overline{Q_{i(j-1)}Q_{ij}}\}$$

Where,  $Q_i$  denotes the  $i$ th obstacle;  $Q_{ij}$  denotes the  $j$ th vertex of the  $i$ th polygon obstacle, where  $1 \leq i \leq j$ , there are  $j$

vertices;  $\overline{Q_{i1}Q_{i2}}$  denotes the connecting line segment of  $Zi1$ 、 $Zi2$  vertex angle of the  $i$ th obstacle.

The position and size of the convex polygon obstacle can be represented by the coordinates of each vertex, namely  $(x_{Qi1}, y_{Qi1})$ ,  $(x_{Qi2}, y_{Qi2})$ ,  $\dots$ ,  $(x_{Qij}, y_{Qij})$ .

Circular obstacles can be expressed as:

$$Q_o = \{Q_{o1}Q_{o2} \dots Q_{oi}\}$$

$$Q_{oi}(x, y) = \frac{(x - x_{Q_{oi}})^2}{R_{Q_{oi}}^2} + \frac{(y - y_{Q_{oi}})^2}{R_{Q_{oi}}^2} - 1$$

Where,  $Q_{oi}$  denotes the  $i$ th circular obstacle;  $Q_{oi}(x, y)$  denotes the edge circle coordinate function of the circular obstacle  $Q_{oi}$ ; the circle center coordinate is  $(x_{Q_{oi}}, y_{Q_{oi}})$ , and the radius is  $R_{Q_{oi}}$ .

Therefore, the position and size of a circular obstacle can be expressed by the center coordinates and radius length.

(2) Trajectory tracking and short-term prediction of dynamic obstacles

According to the position information of each instantaneous obstacle, the historical trajectory of the obstacle can be calculated. Based on the historical trajectory data and the LSTM trajectory prediction model, the short-term prediction of the future trajectory of dynamic obstacles can be realized to further improve the safety and predictability of parking trajectory planning.

The main dynamic obstacles in the parking environment include vehicles, pedestrians, non-motor vehicles, pets, etc. The prediction of obstacles is mainly based on its historical trajectory and intention to predict its future trajectory. In addition, obstacles in the environment have interaction, that is, when the direction of obstacle movement is not affected by

other obstacles, it moves according to its original trajectory trend, and when the direction of obstacle movement is affected by other obstacles, it will correct its own trajectory.

Firstly, the intention recognition of obstacles is based on the LSTM network, that is, based on the historical trajectory of obstacles, the probability of future trajectory of obstacles is calculated. The model structure is shown in Figure 5.

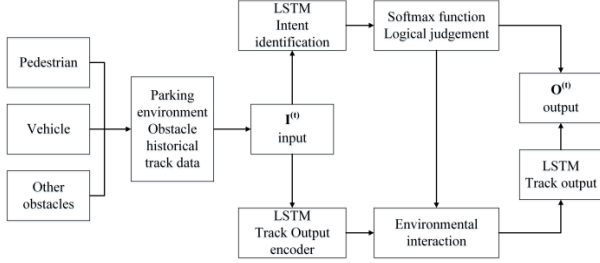


Fig. 5 LSTM trajectory prediction model framework

Assuming that the input of the model is  $I$ , which is the historical trajectory of the obstacle and the rotation angle and environmental information, expressed as :

$$I^{(t)} = [S_e^{(t)}, E^{(t)}] \quad T_p \leq t \leq T$$

Where,  $S_e(t)$  denotes the historical motion trajectory of the predicted obstacle;  $E(t)$  denotes the environmental information, mainly including the motion trajectory of spatially combined and other obstacles and the predicted trajectory;  $T_p$  denotes the historical time domain;  $T$  denotes the whole-time domain.

The output intention category of the intention recognition module is  $U = (u_1, u_2, u_3)$ , where  $u_1$ ,  $u_2$ ,  $u_3$  represent the three intention categories of lateral movement, longitudinal movement and rotation to the obstacle, respectively.  $K = (k_1, k_2, k_3)$  represents the probability of lateral movement, longitudinal movement and rotation to the obstacle, respectively. The output of the intention recognition module is:

$$k_i = P(u_i | I) \quad i = 1, 2, 3$$

The distribution probability of the predicted future trajectory is :

$$p(H | I) = \sum p_{\pi, \mu, \sigma}(H_i | u_i, I) p(u_i | I)$$

Where,  $H$  is the model output;  $P_{\pi, \mu, \sigma}(H_i | u_i, I)$  is the probability distribution of trajectories based on different driving intentions;  $\pi, \mu, \sigma$  are the model calculation parameters.

Environmental information mainly considers the interaction when the predicted trajectory of obstacles conflicts, that is, each obstacle should maintain a certain distance relationship, that is :

$$E^{(t)} = (S_{e_i}^{(t)}, v_{S_{e_i}}^{(t)})$$

$$S_{e_i}^{(t)} = (\Delta x_{e_i}^{(t)}, \Delta y_{e_i}^{(t)}, \Delta \delta_{e_i}^{(t)})$$

Where,  $S_{e_i}(t)$  denotes the predicted motion trajectory of each obstacle in the environment;  $v_{S_{e_i}}(t)$  denotes the predicted motion velocity of each obstacle in the environment;  $\Delta x_{e_i}(t)$ ,  $\Delta y_{e_i}(t)$ , and  $\Delta \delta_{e_i}(t)$  denote the lateral, vertical, and rotational angle variations, respectively.

Therefore, the predicted horizontal and vertical coordinates are:

$$H^{(t)} = [X^{(t)}, Y^{(t)}, \eta^{(t)}] \quad T_p \leq t \leq T$$

Where,  $X$ ,  $Y$ , and  $\eta$  denote the horizontal and vertical coordinates and angular sequences, respectively.

### 3.1.2. Obstacle collision analysis

The vehicle and the obstacle are projected on the two-dimensional plane. When the overlap area between the vehicle and the obstacle is greater than 0, the vehicle collides. The vehicle collision diagram is shown in Figure 6, where the blue rectangular frame represents the vehicle, the red rectangular frame and the circle represent the obstacle, and the light blue or yellow part of the outer side is the expansion part.

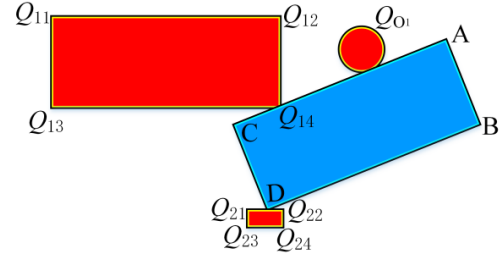


Fig. 6 Vehicle collision diagram

It can be seen from the above figure that when the obstacle is a convex polygon, the collision of the vehicle must originate from the vertex. The triangle area method can be used to further determine whether the vertex collides, that is, a point  $Q$  outside the convex polygon is connected to the vertices of the convex polygon. If the sum of the triangle areas formed by  $Q$  and each two adjacent vertices of the convex polygon is greater than the sum of the convex polygons, then the  $Q$  point is located outside the convex polygon. With  $Q_{ij}$  representing the vertices of the polygon obstacle, the vehicle vertices  $A, B, C, D$ , and  $Q_{ij}$  should satisfy:

$$\begin{cases} S_{\Delta Q_n AB} + S_{\Delta Q_n AC} + S_{\Delta Q_n BD} + S_{\Delta Q_n CD} > S_{ABCD} & 1 \leq n \leq j \\ S_{\Delta Q_i Q_j} + \sum_{n=1}^{j-1} S_{\Delta Q_n Q_{i(n+1)}} > S_{Q_i} & \chi = \{A, B, C, D\} \end{cases}$$

Where,  $S_{Q_i}$  denotes the area of the convex polygon obstacle  $Q_i$ ,  $j$  denotes the number of vertices of the obstacle  $Q_i$ ,  $n$  denotes the  $n$ th vertex of the obstacle  $Q_i$ , and  $\chi$  denotes the ensemble of vehicle vertices  $A, B, C$ , and  $D$ .

When the obstacle is circular, the distance between any point on the vehicle and the circle should be greater than its radius to ensure that no collision occurs, then the vehicle vertices  $A, B, C, D$  should meet:

$$\min \left( \sqrt{(x - x_{Q_{0i}})^2 + (y - y_{Q_{0i}})^2} \right) > R_{Q_{0i}}$$

Where,  $(x, y)$  denotes a point on the edge of the vehicle,  $(x_{Q_{0i}}, y_{Q_{0i}})$  denotes the coordinates of the circle center of the circular obstacle  $Q_{0i}$ , and  $R_{Q_{0i}}$  denotes the radius of the circle  $Q_{0i}$ .

### 3.2. Optimal vertical parking path planning considering the influence of obstacles

First, according to the parking space, the initial position and attitude of the vehicle information, obstacle information, select all parking strategies that meet the constraints. When the vehicle is parked vertically, if there may be a conflict with the dynamic obstacle trajectory, three obstacle avoidance methods can be used to ensure the safe and successful parking of the vehicle, including parking waiting, changing the parking strategy and adjusting the vehicle position to re-plan the path.

The selection of obstacle avoidance mode in vehicle parking process mainly considers the parameters such as size, shape and future trajectory of dynamic obstacles. The

selection of different scenarios is shown in Figure 7.

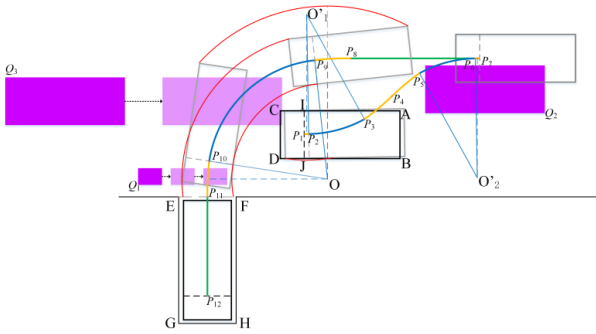


**Fig. 7** Parking strategy and obstacle avoidance choice under different scenarios

When the obstacle and the vehicle may conflict at the parking space, such as obstacle Q1, the vehicle can only choose to park and wait for obstacle avoidance; when the obstacle is located in front of the initial position of the vehicle, such as obstacle Q2, the vehicle can only use one parking strategy or multiple adjustment parking strategy, that is, when the vehicle forward adjustment parking strategy is selected to change the parking strategy to achieve obstacle avoidance; when the obstacle is located in the middle of the lane, it may conflict with the vehicle and occupy the target channel with each other, that is, the vehicle and the obstacle cannot continue to travel according to the original planned route. For example, obstacle Q3, the obstacle avoidance method of re-planning the path by adjusting the vehicle position is selected, that is, the vehicle stops parking and goes forward to the roadside. After the obstacle passes, the parking strategy is re-selected for parking.

The optimal selection of parking paths for different parking strategies and different obstacle avoidance methods mainly considers the path efficiency, that is, the time required for the vehicle to be parked in the process. The whole process of parking is taken as a specific evaluation index, and the path with the smallest evaluation index is selected as the optimal parking path. The evaluation index expression is:

$$M = \sum_{i=1}^j \frac{L_i}{\bar{v}_i} + k_n N + T$$

Where, M is the quantitative evaluation index;  $L_i$  is the length of the  $i$ th line segment;  $\bar{v}_i$  is the average speed of the line segment; the whole process of parking a total of  $j$  line segments;  $k_n$  is the vehicle turning time consumption coefficient,  $N$  is the number of vehicles turning,  $T$  is the parking waiting time when the vehicle is parked.

#### 4. Simulation analysis

The parking path planning algorithm is simulated and verified in QT environment. It is assumed that the vertical parking space is 5.5 m in length and 2.4 m in width, which is a narrow parking space. The vertical parking path of the vehicle is planned. The three parking path planning strategies are simulated in Figure 8, Figure 9 and Figure 10, where the blue curve represents the rear axle driving path of the vehicle. The simulation diagram of vertical parking path planning after adding obstacle prediction is shown in Figure 11.

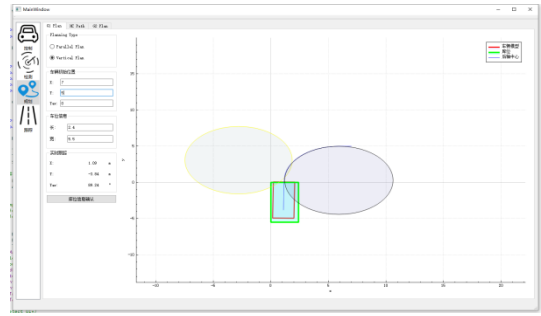


**Fig.8** Vehicle parking strategy simulation

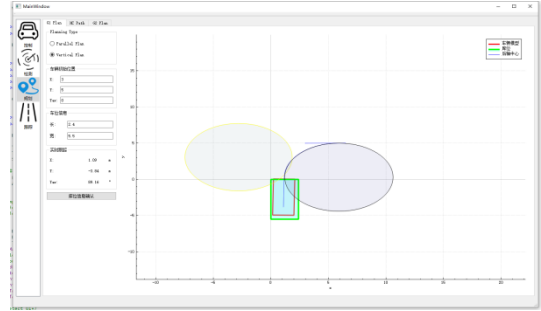


**Fig. 9** Simulation of reverse parking strategy after vehicle forward adjustment

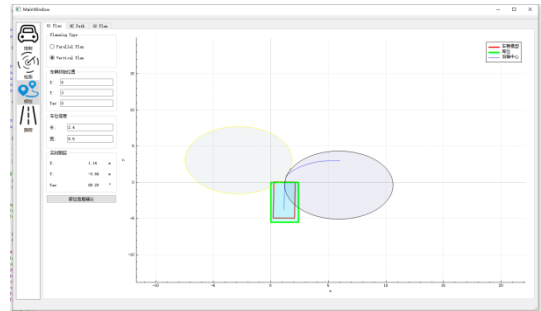


**Fig.10** Simulation of vehicle multiple adjustment parking strategy

The simulation results show that when the parking space environment and the initial position of the vehicle are different, the three vertical parking path planning strategies based on the arc-straight line-relaxation curve can effectively plan the vertical parking path and greatly improve the safety and success rate of parking path planning.

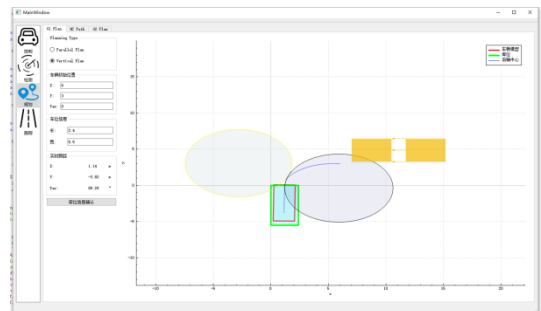


**Fig. 11** Simulation of vehicle vertical parking considering obstacles

From the simulation results of the vertical parking path with obstacles, it can be seen that by predicting the future trajectory of obstacles, the obstacle avoidance method of changing the parking strategy is adopted, and the reverse parking strategy after the vehicle forward adjustment is adjusted to the vehicle multiple adjustment parking strategy, which realizes safe obstacle avoidance and efficient parking.

## 5. Conclusion

In this paper, the parking path planning of narrow vertical parking space is studied. Considering the complexity and variability of parking environment, the parking with high success rate, high safety, strong adaptability and good efficiency is realized. The main tasks are as follows:

(1) Multi-strategy parking path planning under different vehicle initial positions and postures. Using the path planning method of arc-line-transition curve, and using three planning strategies of one-time parking, reverse parking after vehicle forward adjustment and multiple adjustment parking, the parking of continuous curvature path under different positions and postures of vehicles is realized.

(2) Predictive parking path planning considering obstacle prediction trajectory. Considering the complex influence of obstacles in parking environment, considering the historical trajectory and interaction of obstacles, the future trajectory of obstacles is predicted, and three parking obstacle avoidance methods are proposed to realize safe and efficient path planning in different parking environments.

(3) Optimal path planning selection. Combined with different initial positions and postures of the vehicle and obstacle information, three planning strategies and three obstacle avoidance methods are used to achieve the optimal parking path planning with parking time as the evaluation index.

## References

- [1] Paul Green. Parking Crashes and Parking Assistance System Design: Evidence from Crash Databases, the Literature and Insurance Agent Interviews [J]. SAE World Congress, 2006, 1:1685-1700.
- [2] SHOUP D C. Cruising for parking [J]. Transport Policy, 2006,13(6):479-486.
- [3] LI X H. Research on automatic parking path planning and tracking control in narrow parking spaces[D]. Dalian: Dalian University of Technology, 2021.
- [4] CHAI R, TSOURDOS A, SAVVARIS A, et al. Multi-objective optimal parking maneuver planning of autonomous wheeled vehicles[J]. IEEE Transactions on Industrial Electronics, 2020, 67(12):10809-10821.
- [5] BERGMAN K, LJUNGVIST O, AXEHILL D. Improved path planning by tightly combining lattice-based path planning and numerical optimal control[J]. 2019, arXiv:1903.07900.
- [6] ZHANG J, CHEN H, SONG S, et al. Reinforcement learning based motion planning for automatic parking system[J]. IEEE Access, 2020, 8:154485-154501.
- [7] MAHESHWARI S, MAHAPATRA S, KUMAR C S, et al. A Joint Parametric Prediction Model for Wireless Internet Traffic Using Hidden Markov Model [J]. Wireless Networks, 2013, 19(6):1171-1185.
- [8] QIAO Shao-jie, HAN Nan, ZHU Xin-wen, et al. Dynamic Trajectory Prediction Algorithm Based on Kalman Filter [J]. Acta Electronica Sinica, 2018, 46(2):418-423.
- [9] QIAO Shao-jie, JIN Kun, HAN Nan, et al. A Trajectory Prediction Algorithm Based on Gaussian Mixture Model [J]. Journal of Software, 2015(5):76-91.
- [10] PAN J, SUN H, XU K, et al. Lane-Attention: Predicting Vehicles' Moving Trajectories by Learning Their Attention Over Lanes[C]//2020 IEEE/RSJ International Conference on Intelligent Robots and Systems (IROS). IEEE, 2020:7949-7956.
- [11] JITENDRA K, RIMSHA G, ASHUTOSH K S. Long Short Term Memory Recurrent Neural Network (LSTM-RNN) Based Workload Forecasting Model For Cloud Datacenters [J]. Procedia Computer Science, 2018, 125:676-682.
- [12] ZHANG J F, ZHU Z, ZHANG X P, et al. Developing a Long Short-term Memory (LSTM) Based Model for Predicting Water Table Depth in Agricultural Areas [J]. Journal of Hydrology, 2018, 561:918-929.